



Autothermal reforming of JP8 on a Pt/Rh catalyst: Catalyst durability studies and effects of sulfur

Naomi B. Klinghoffer, Federico Barrai, Marco J. Castaldi*

Department of Earth and Environmental Engineering, Columbia University, New York, NY 10027, USA

ARTICLE INFO

Article history:

Received 23 January 2011

Received in revised form 27 February 2011

Accepted 28 February 2011

Available online 6 March 2011

Keywords:

Autothermal reforming

Sulfur

Jet fuel

Fuel processor

Catalyst deactivation

Hydrogen

ABSTRACT

Autothermal reforming (ATR) of commercial grade JP8 was performed on a Pt/Rh catalyst deposited on a monolith. This study investigated catalyst performance under three test conditions: (i) 120 startup and shutdown cycles, (ii) 80 h of continuous operation with sulfur-free fuel, and (iii) 370 h of testing with JP8 containing 125 ppm of sulfur. Axial reactor temperature profiles and gas composition data showed that startup and shutdown cycling had no impact on catalyst performance. When durability testing was done with fuel containing 125 ppm of sulfur, the catalyst deactivated initially, which was reflected by a decrease in H₂ concentration and decrease in fuel conversion. However, after 250 h of operation the activity stabilized at 66% fuel conversion and product concentrations were constant for the remaining 120 h of testing. The presence of sulfur resulted in higher CO selectivity, lower H₂ concentrations, and lower fuel conversions compared to data with sulfur-free fuel. The data suggests that the presence of sulfur primarily affects steam reforming reactions, and CO oxidation. Regeneration was attempted with air and with fuel-lean combustion but initial H₂ yields and carbon selectivity were not achieved.

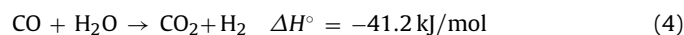
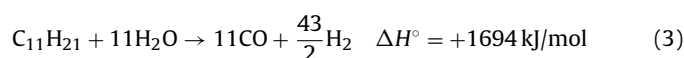
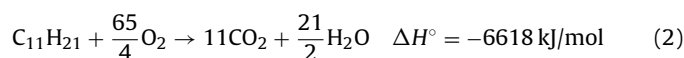
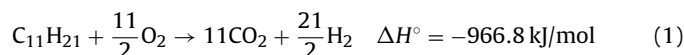
© 2011 Elsevier B.V. All rights reserved.

1. Introduction

The production of hydrogen or synthesis gas on a distributed scale is being investigated for a variety of applications. Possible uses range from power production in fuel cells, combustion enhancements for higher power or emission reductions, or chemical synthesis. Synthesis gas can be obtained from the thermal or catalytic decomposition of a wide range of organic materials such as hydrocarbons, biomass, or waste. For the special case of distributed applications, a liquid fuel is most convenient due to the presence of a well-developed infrastructure for its delivery and its high energy density compared to other fuels. JP8 (Jet Propulsion 8) is a commonly used liquid fuel and is therefore widely distributed, making it a good candidate for portable power applications.

The main catalytic methods for generating synthesis gas from liquid fuels, such as JP8, are partial oxidation (POX), steam reforming (SR), and auto-thermal reforming (ATR). Partial oxidation is an exothermic reaction, where the oxygen (usually from air) to fuel ratio is sub-stoichiometric for combustion, and produces H₂/CO ratios dictated by the H/C ratio of the fuel itself. POX reactors produce very high temperatures and have some degree of complete

oxidation which reduces the hydrogen yield [1]. SR can produce much higher H₂/CO ratios compared to POX since hydrogen is added to the fuel via water [2]. Additionally, the product stream has a higher energy density since N₂ dilution (from the addition of air) does not exist. However, steam reforming is an endothermic reaction that, combined with the evaporation of the steam, can have high energy requirements [2]. ATR combines POX and SR by introducing a mixture of oxidant, fuel, and steam into a catalytic reactor. This enables tuning of the H₂/CO ratio with a higher degree of freedom compared to POX and SR (by adjusting both steam to carbon and oxygen to carbon ratios) and eliminates the need for external heating. The overall process can be simplified by designating three types of reactions: oxidation reactions, water consuming reactions, and fuel cracking reactions. Oxidation reactions include partial and complete oxidation (see Eqs. (1) and (2)). Water consuming reactions include steam reforming of fuel and water gas shift (WGS) reaction (see Eqs. (3) and (4)). Cracking of the fuel has been shown to take place during ATR of large hydrocarbons [3,4]. The reactions shown here use C₁₁H₂₁ as a representative model for JP8.



* Corresponding author. Present address: Department of Earth and Environmental Engineering, 918 S.W. Mudd Hall, 500 West 120th Street, New York, NY 10027, USA. Tel.: +1 212 854 6390; fax: +1 212 854 7081.

E-mail addresses: nbk2107@columbia.edu (N.B. Klinghoffer), mc2352@columbia.edu (M.J. Castaldi).

Typically the ATR reactor features an oxidation zone at the upstream end, and a reforming zone downstream, which results in a temperature gradient where there are high temperatures in the upstream portion of the catalyst bed [5].

Catalysts are routinely used in industrial applications primarily on a large scale and in stationary processes. The introduction of catalysts into portable applications presents new challenges. For example, portable applications will involve frequent startups and shutdowns which introduce thermal cycling of the catalyst. Additionally, in ATR, fuel and steam are introduced into the reactor when it is at a low temperature (300–400 °C) before the reactor lights off. It has been shown that for some catalysts, specifically copper based catalysts, frequent startups and shutdowns can lead to catalyst deactivation [6,7]. Gould et al. observed temperature excursions during startup of an ATR reactor with jet fuel, while using a nickel–ceria–zirconia based catalyst, which caused sintering of the catalyst support [8]. Therefore, the research presented in this paper includes startup and shutdown cycling in order to observe impacts from these procedures on this catalyst's performance. Furthermore, in portable applications, it is desirable to minimize routine maintenance therefore the catalyst should have stable long term activity. Catalysts can deactivate over time via three primary deactivation mechanisms which are coking (carbon deposition on the catalyst), poisoning (deposition of a species on the catalyst surface or reaction of a species with the catalyst or carrier) or sintering of the catalyst or carrier [9–12]. Moreover, sulfur is a known catalyst poison, therefore if sulfur is present in a fuel it is important to consider its impact on catalyst performance [9,13,14].

The fuel tested in this study was JP8 which includes a mix of hydrocarbons (C9–C17+), various aromatic and aliphatic compounds [15], and can contain up to 0.3 wt.% sulfur [16]. Additionally, most commercial grade JP8 often contains additives such as corrosion inhibitors, static dissipaters, and icing inhibitors [16]. It is common in literature on ATR of commercial fuels such as JP8 or diesel to use surrogates such as n-dodecane, tetralin or n-hexadecane [8,17–19]. Using surrogates allows for a more detailed understanding of reaction mechanisms, measurement of fuel conversions, and allows for modeling work to be done since thermodynamic properties of pure hydrocarbons are available. However, aromatics can be more difficult to reform and therefore, in experimental work conversion may be artificially enhanced if straight chain hydrocarbons are used to model fuels with aromatics [20,21]. Additionally, H₂ selectivity has been shown to be slightly lower for straight chain hydrocarbons than for aromatics (straight chain hydrocarbons can crack which results in smaller gas phase hydrocarbons whereas aromatics are more likely to get reformed to H₂) [20]. Flytzani-Stephanopoulos et al. performed ATR with aliphatics and with aromatics on a supported nickel catalyst and found that aromatics have less fuel cracking in the entrance, slower steam reforming reactions, and less surface carbon formation than aliphatics [22]. Therefore, this work has been done using commercial grade JP8 fuel to give a realistic representation of catalyst performance.

JP8 often contains sulfur which has been shown to decrease H₂ yields, increase CO selectivity, and decrease overall fuel conversion [13,18,20]. However, regeneration is possible following catalyst deactivation in the presence of sulfur. Qi et al. [20] showed that nearly all of the catalyst activity could be recovered during ATR of gasoline on a Rh-based monolithic catalyst by introducing sulfur-free fuel following 25 h of operation with sulfur-laden fuel. Ferrandon et al. [9] observed the same effects with a Rh catalyst (catalyst activity recovery from introducing sulfur-free fuel), and found that temperatures of at least 800 °C were necessary in order to achieve complete recovery of catalyst activity. Cheekatamarla et al. [13] showed that during ATR of diesel fuel with a Pt/ceria catalyst some of the catalyst activity was recovered after sulfur

poisoning, but initial H₂ yields were not achieved when cycling between sulfur-free and sulfur-containing fuel.

While regeneration can significantly enhance the lifetime of the catalyst, ideal working conditions would allow for continuous catalyst use without the need for regeneration. There is limited literature that examines long-term continuous ATR operation with sulfur present. Lee et al. conducted 96 h of ATR using JP8 containing 1096 ppm of sulfur on a Rh-alumina foam catalyst and observed significant and continuous deactivation [23]. Cheekatamarla et al. found that with a Pt/Pd catalyst the H₂ yield decreased from 78% to 55% over 50 h of ATR with synthetic diesel containing 1000 ppmw of sulfur [24]. Pasel et al. were able to achieve high catalyst performance during ATR for 2000 h of operation using desulfurized Jet A-1 [25]. Qi et al. have performed ATR on a Rh-based catalyst with sulfur-free iso-octane for 1000 h and observed significant deactivation after 800 h [26]. Since many fuels are not sulfur-free, it was of interest to us to attempt to find stable catalyst performance over long periods of time using sulfur-laden fuel.

2. Materials and methods

2.1. Experimental setup

Feed delivery system and reactor. A diagram of the experimental setup is shown in Fig. 1. The catalyst was a Pt/Rh based formulation provided by BASF (catalog #RM-75ST) which was deposited onto a 400 cpsi (62 cells cm⁻²) cordierite monolith support with a washcoat loading of 2 g in.⁻³ (0.12 g cm⁻³). The coated monolith was 3/4 in. (1.9 cm) diameter and 4.2 in. (10.7 cm) in length. The reactor apparatus was equipped with 10 K-type thermocouples (0.5 mm diameter, inconel sheath, Omega KMQIN-010U-24) introduced radially, which were distributed axially at equal distances (approximately every 1 cm) along the monolith. The reactor was well insulated and no external heating was applied to the reactor. Water was introduced into the steam generator via an in-house built pump. The flow rate of water was controlled with a needle valve (Swagelok SS-SS4) and measured with a rotameter (Gilmont GF-2100). A two-stage steam generator was used where the first heater evaporated the water and the second steam generator superheated it to 350 °C. The JP8 was introduced via a rotating-reciprocating piston pump (FMI PDS-100) and the flow rate was checked with a rotameter (Omega 3461C) downstream of the pump. The JP8, which was at room temperature, was mixed with the superheated steam exiting the second steam generator which evaporated the fuel. The fuel/steam mixture was then mixed with pre-heated air (300 °C) and the air/fuel/steam mixture was heated to the desired inlet temperature and then introduced into the reactor.

Product analysis. A Teflon lined piston pump was used to draw a sample from the exhaust stream for analysis with the remaining exhaust vented. The sample was passed through a condenser, maintained at 0 °C by an ice/water reservoir (for sulfur-free experiments) or 22 °C by a continuous flow of tap water (for 125 ppm sulfur experiments) in order to remove water and condensable hydrocarbons. A gas chromatograph (Agilent micro GC 3000A) was used to analyze gas-phase products. The products were measured with a Molecular sieve column and a Plot-U column coupled to a thermal conductivity detector.

2.2. Experimental conditions

The goal of this test campaign was to understand how catalyst activity is impacted by (i) startup and shutdown cycles, (ii) long term continuous operation in the absence of sulfur, and (iii) long term continuous operation in the presence of sulfur. For each of

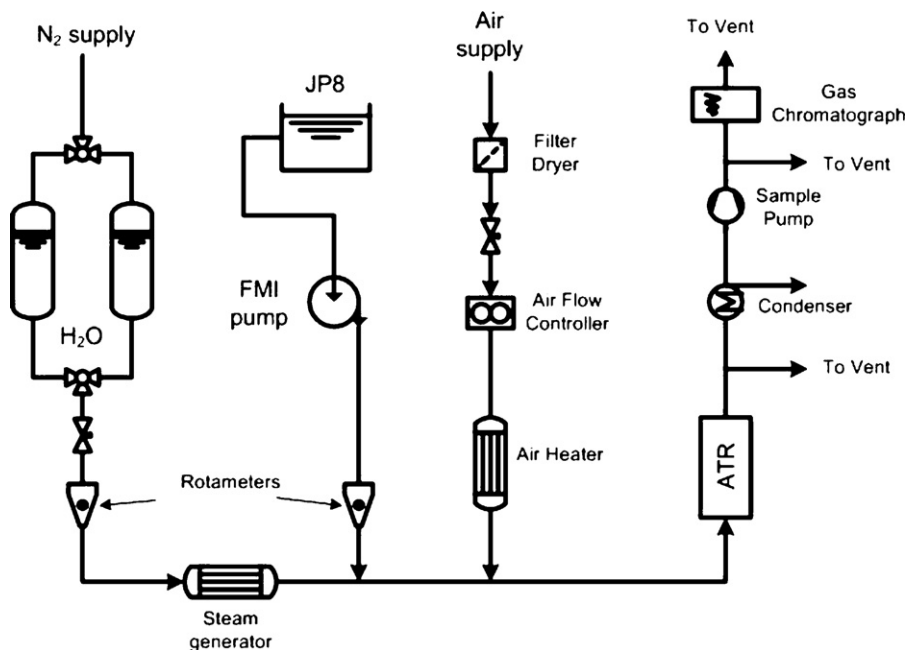


Fig. 1. A simplified process flow diagram of the experimental apparatus used for ATR.

these three tests a fresh catalyst was used. For the sulfur-free testing, commercial grade desulfurized JP8 was used. For the testing with sulfur present, non-desulfurized commercial grade JP8 was mixed with sulfur-free JP8 in order to achieve a final sulfur concentration of 125 ppm in the fuel (the final sulfur concentration was measured). The specific form of sulfur in the fuel can vary depending on how the crude is processed, however sulfur in JP8 is typically in the form of thiophenes. For example, Nair and Tatarchuk measured a high concentration of tri-methyl benzothiophene in JP8 [27]. The cycle testing consisted of 120 startups and shutdowns. For each cycle, the reactor was heated to 300 °C with steam, and subsequently fuel was introduced, followed by air, which initiated reaction. The reactor temperatures and output gases were monitored continuously until steady state was achieved. Next air and fuel were shut off, while water was left on at nominal conditions. The reactor was cooled to 300 °C with room temperature air before beginning the next cycle. Nominal conditions were a steam to carbon ratio (S/C) of 1.0, oxygen to carbon ratio (O/C) of 1.0 and a gas hourly space velocity (GHSV) of 30,000 h⁻¹. These cycle tests were conducted with sulfur-free fuel (<1 ppm of sulfur). Next, a durability test was run with sulfur-free fuel; the reactor was run for 80 h continuously at a S/C of 1.4, an O/C of 0.9, and a GHSV of 29,000 h⁻¹. Durability testing in the presence of sulfur was conducted with fuel containing 125 ppm of sulfur at the same conditions (S/C 1.4, O/C

0.9, GHSV 29,000 h⁻¹) for a total of 370 h; initially short-term tests were done (about 3–15 h each, for a total of 28 h), after which ATR was run for 50 h, and then 300 h continuously (all on the same catalyst). During the tests reactor temperatures, inlet temperature, and gas concentrations were measured. Regeneration of the catalyst was attempted and is discussed in detail in Section 3.4.

2.3. Calculations

Fuel conversion. Fuel conversion was calculated based on the amount of carbon from the fuel which was converted into a gas phase carbon based product (CO, CO₂, CH₄, C₂ species). Conversion was defined this way because the objective of this system is to convert liquid fuel to synthesis gas. Therefore any liquid products (for example, cracked fuel) result in reduced conversion. Using N₂ as an internal standard and measured mole fractions of all gas phase species, the flow rate of products exiting the reactor in the gas phase was calculated. This was verified via an oxygen balance which included the liquid phase products. Using an assumption that all oxygen in the condensed phase was in the form of water (no alcohols, esters, etc. in the condensed phase), flow rate of water in the reactor exhaust was calculated by an oxygen balance. During experiments, the volumetric ratio of water to hydrocarbons in the condenser was measured. This allowed us to calculate the flow

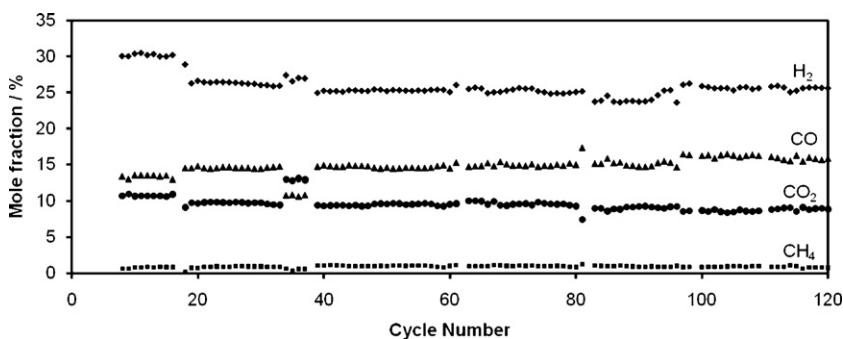


Fig. 2. Product concentrations for H₂ (◆), CO (▲), CO₂ (●), and CH₄ (■) during cycle testing with sulfur free JP8. For cycles 35–38, S/C=2; all other cycles are at nominal conditions of S/C=1, O/C=1 and GHSV=30,000 h⁻¹.

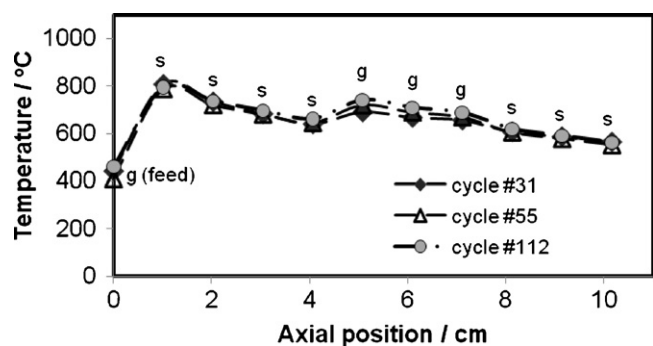


Fig. 3. Temperature profiles in reactor during cycle testing ($S/C=1$; $O/C=1$; $GHSV=30,000\text{ h}^{-1}$). *S* indicates that the temperatures are measured at the catalyst wall; *g* indicates gas phase temperatures.

rate of hydrocarbons exiting the reactor based on this ratio and on the water flow rate. JP8 conversion was calculated on a volumetric basis, as shown in Eq. (5). Both methods gave conversion values within 5% of each other, confirming that this calculation is aligned with the overall carbon balance for this system. With JP8 it is difficult to completely close the carbon balance, therefore we could not directly measure carbon formation on the surface. However, experimental data was used to understand if carbon formation was taking place.

$$\text{Fuel conversion} = \frac{\text{JP8 in (ml/min)} - \text{liquid hydrocarbons out (ml/min)}}{\text{JP8 in (ml/min)}} \quad (5)$$

Equilibrium concentrations. To determine the proximity of the reactor conditions to equilibrium product distribution, equilibrium product distributions were calculated using Gaseq. Gaseq is a program that calculates equilibrium concentrations by minimizing Gibbs free energy. All equilibrium concentrations presented here were calculated with Gaseq at all measured reactor temperatures and atmospheric pressure. Reactant concentrations were set equal to those of the experimental system and products were said to be measured gas phase species (from experiments), water, and fuel. JP8 properties were manually added to the thermodynamic database of Gaseq. Concentrations presented in this paper are on a dry basis.

3. Results and discussion

3.1. Sulfur-free fuel – cycle testing

In portable applications ATR reactors will be subjected to frequent start-ups and shut-downs. The objective here was to determine the performance impact from frequent startup and shut-down cycles. This was tested by performing 120 reactor cycles and

continuously measuring the product distribution and temperature profile to observe the stability throughout testing. Steady state product distributions for each cycle that was completed at nominal S/C , O/C and $GHSV$ are shown in Fig. 2. Cycles that are missing were done at different conditions and for simplicity are not shown on this graph. The first set of cycles was done at a slightly higher reactor temperature (front end reactor temperature was $815\text{ }^\circ\text{C}$ instead of $790\text{ }^\circ\text{C}$), which resulted in higher H_2 and CO production, and lower CO_2 (compared to other cycles). Subsequently product concentrations were stable; H_2 concentration remained within 5% of the initial value and CO and CO_2 concentrations remained within 8% of initial values for a given reactor temperature. For cycles #35–38, the S/C ratio was increased from 1 to 2 to determine the effect of changing process conditions on catalyst performance. This resulted in a decrease in reactor temperature as more steam was introduced. In Fig. 3 the temperature profiles in the reactor are shown during three different cycles, near the beginning, middle, and end of testing (cycles #31, 55, 112). For all tests done at nominal conditions, measured temperatures were within 7% of each other at all reactor locations, indicating stable catalyst activity throughout cycle testing. Therefore, both temperature data and product concentration data indicate that the startup and shutdown procedure does not impact catalyst performance. This is important when using catalyst in portable applications when startup and shutdown are very frequent.

When the S/C was increased from 1 to 2 (cycles 35–38), the selectivity of carbon species favored CO_2 over CO , as shown in Fig. 2. Simultaneously, H_2 increased from 26% to 28%, CO decreased from 15% to 11% and CO_2 increased from 10% to 13%. At a S/C ratio of 1, the maximum reactor temperature was $790\text{ }^\circ\text{C}$ (exit temperature $555\text{ }^\circ\text{C}$) and for a S/C ratio of 2, the maximum reactor temperature was $730\text{ }^\circ\text{C}$ (exit temperature $530\text{ }^\circ\text{C}$). Measured product concentrations most closely matched equilibrium values calculated at the maximum measured reactor temperature rather than downstream temperatures, as shown in Fig. 4, indicating that front end reactor temperature is important in determining final product distribution. According to thermodynamics, a higher S/C ratio gives higher concentrations of H_2 and CO_2 and lower concentrations of CO , which is likely caused by a shift in the equilibrium of the WGS reaction. Lower reactor temperature leads to lower concentrations of H_2 and CO and higher CO_2 concentration. In this experiment, an increase in S/C resulted in lower reactor temperatures, therefore when S/C was increased from 1 to 2 the hydrogen increased by 1% rather than the 3% expected increase if the reactor were operated at the same temperature. For both S/C ratios, CO and CO_2 concentrations

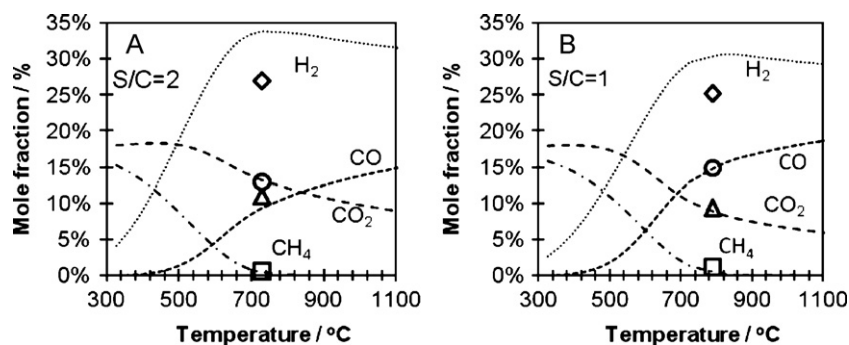


Fig. 4. Calculated equilibrium product concentrations (lines) and measured values (data points) for (A) $S/C=2$; (B) $S/C=1$. Measured product concentrations are plotted at maximum reactor temperature.

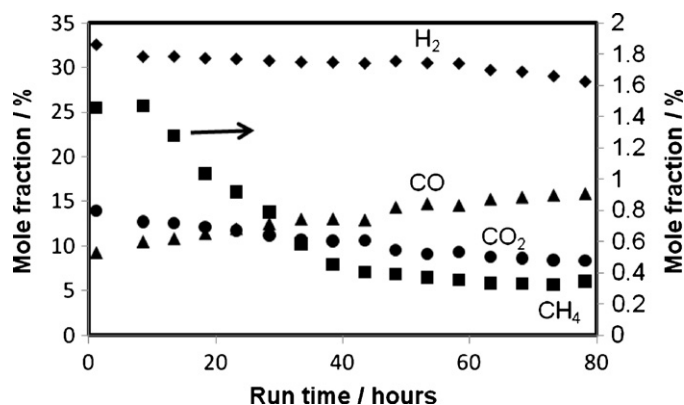


Fig. 5. Product concentrations for H₂ (◆), CO (▲), CO₂ (●), and CH₄ (■) during durability testing with sulfur-free fuel. S/C = 1.4, O/C = 0.9 and GHSV = 29,000 h⁻¹.

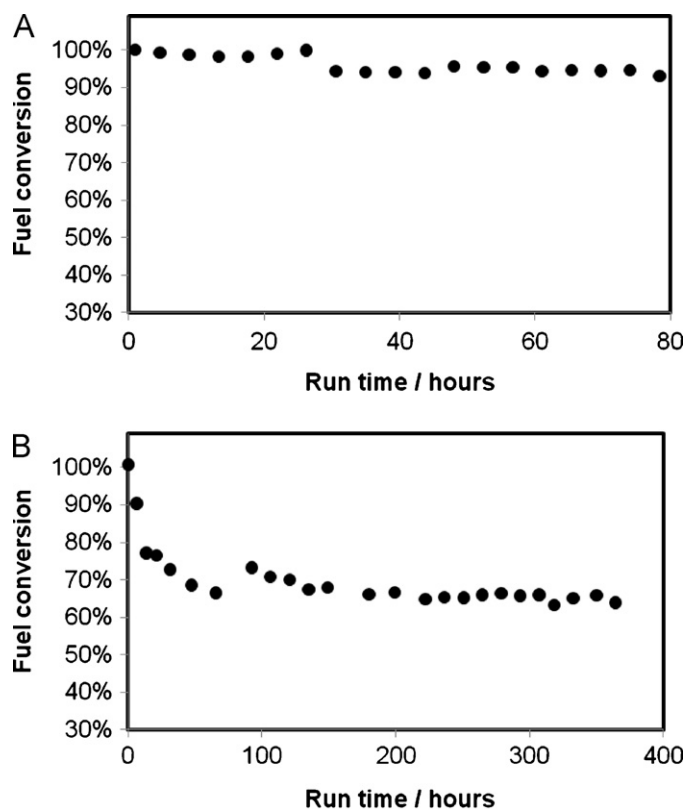


Fig. 6. Fuel conversion during durability test with (A) sulfur-free fuel; (B) 125 ppm sulfur in fuel. S/C = 1.4, O/C = 0.9, and GHSV = 29,000 h⁻¹.

are aligned with equilibrium calculations within 1.5%. H₂ concentrations are farther from equilibrium values, yet they still follow the expected trend (H₂ increased by 1% according to both measurements and calculations that account for temperature changes). It has been reported in literature [3,4] that H₂O is primarily consumed via reactions with cracked hydrocarbon species (in other words, JP8 cracks upstream and these smaller hydrocarbons subsequently react with H₂O downstream). Therefore it is possible that kinetics downstream are too slow (at this reactor temperature) to facilitate reaction of all of the steam.

3.2. Sulfur-free fuel – durability test

The product distribution and fuel conversion from 80 h of ATR with sulfur-free JP8 are shown in Figs. 5 and 6A, respectively. Con-

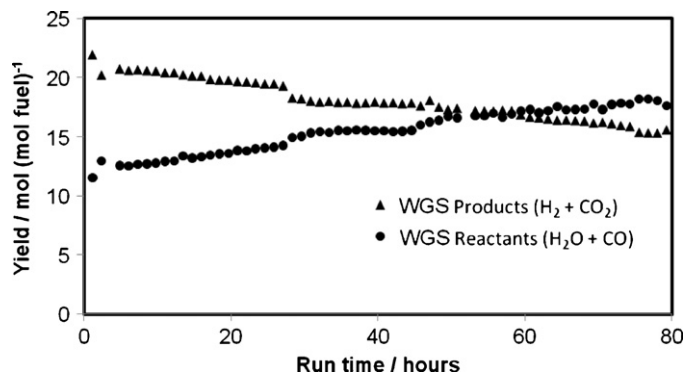


Fig. 7. Yield of WGS reactants (●) and products (▲) during ATR testing with sulfur-free fuel. S/C = 1.4, O/C = 0.9, and GHSV = 29,000 h⁻¹.

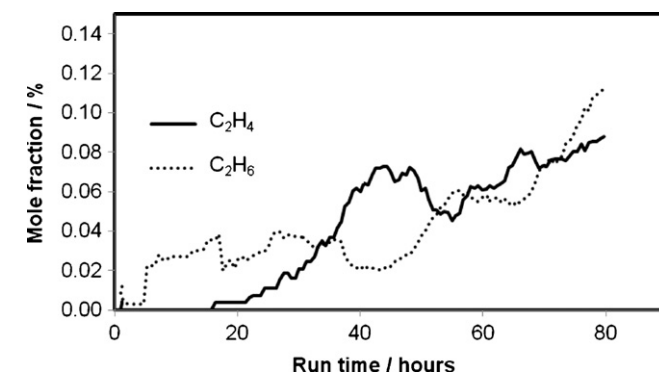
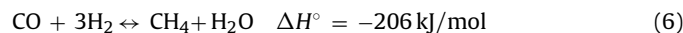


Fig. 8. Concentrations of C₂ species during ATR with sulfur-free JP8. S/C = 1.4, O/C = 0.9, and GHSV = 29,000 h⁻¹. Data is plotted as a moving average over 1 h.

version is initially close to 100% and decreases slightly during the experiment, stabilizing around 93%. While conversion remains relatively stable, selectivity of carbon species switches from CO₂ to CO over time. This could be indicative of a decrease in water gas shift activity, since the water gas shift reaction consumes CO and H₂O, producing CO₂ and H₂. The H₂O concentration exiting the reactor was calculated based on an oxygen balance in the system and a plot of WGS reactants (H₂O + CO) and WGS products (CO₂ + H₂) over the course of the experiment is shown in Fig. 7. Both trends have the same slope (with opposite signs), indicating that the increase in reactant concentration matches the decrease in product concentration. Therefore, it is likely that the WGS reaction is the main reaction impacted by catalyst deactivation during ATR in the absence of sulfur.

CH₄ concentration decreased during the test, as shown in Fig. 5. It is possible that CH₄ is both produced and consumed in the ATR reactor. Rabe et al. observed that during ATR of gasoline, methane is formed in the reactor and the likely mechanism is the methanation reaction (Eq. (6)) [28]. However, Fig. 4 shows that for S/C of 1 measured CH₄ concentrations are almost two times the calculated equilibrium value. Therefore it is possible that CH₄ that is formed (via methanation or cracking) would be consumed by steam reforming if the system was allowed to reach equilibrium. Data for fuel with sulfur presented later in this paper provides further evidence.



The concentrations of light hydrocarbons (C₂H₄ and C₂H₆) were measured throughout the test and a plot of these concentrations is shown in Fig. 8. Measured concentrations of C₂H₄ and C₂H₆ were undetectable at the beginning of the test and increased over time. The increase in smaller hydrocarbons could indicate that more fuel

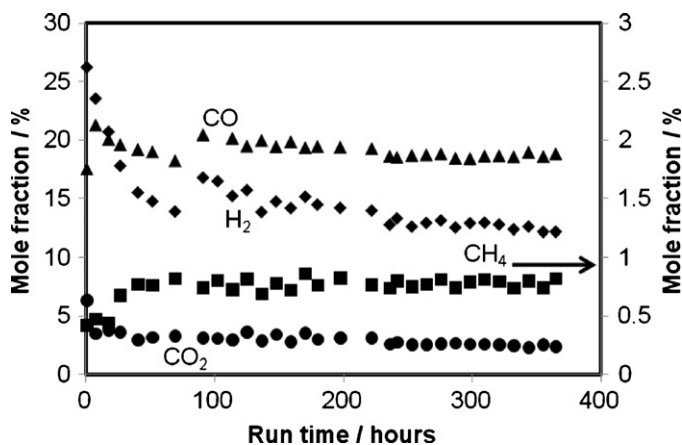


Fig. 9. Product concentrations for H₂ (◆), CO (▲), CO₂ (●), and CH₄ (■) during 370 h of ATR with fuel containing 125 ppm of sulfur. S/C=1.4, O/C=0.9, and GHSV=29,000 h⁻¹.

cracking reactions are taking place (in other words, the fuel is reacting via cracking rather than reforming or oxidation reactions) as the catalyst deactivates. It could also be due to a decrease in steam reforming reactions, which may consume the cracked hydrocarbons to form H₂ and CO (or CO₂).

3.3. 125 ppm sulfur – durability test

ATR was run for 370 h with fuel containing 125 ppm of sulfur and the product distribution is shown in Fig. 9. During the first 28 h of testing, a series of short term tests were conducted to identify acceptable reactor conditions for durability testing. During this time, significant changes in catalyst performance were observed, specifically reflected in the H₂ concentration which decreased by 35% of its initial value. This rapid deactivation is related to the presence of sulfur, since such a rapid deactivation is not observed with sulfur-free fuel. The reactor was shut down after 80 h of operation, and started up again. At this point, regeneration was performed and specific details of this will be discussed in Section 3.4. The last 300 h of the test consisted of continuous operation.

While deactivation was observed at the beginning of the test, the catalyst demonstrated stable performance after 250 h of testing, at which point reactant conversion and product distribution did not change for the remaining 120 h of the test. Applications using this fuel (containing approximately 125 ppm of sulfur) should be designed to accommodate this stable performance. This phenomenon of rapid deactivation followed by stable catalyst performance provides some insight into the deactivation mechanism taking place because it implies that in this system a maximum extent of deactivation exists. Therefore, if the primary deactivation mechanism is sulfur deposition on the surface, then this steady state condition may represent the point when an equilibrium is established between the gas phase sulfur concentration and the surface concentration of sulfur. In other words, sulfur does not continually deposit on the surface otherwise a decline in activity would be observed. Another possible deactivation mechanism is carrier sintering; if this is the primary deactivation mechanism then the steady performance condition may represent the point where stable particle size is achieved, thus no more deactivation is observed.

3.4. Regeneration during testing with 125 ppm sulfur fuel

While the catalyst could be used for long periods of time in its partially deactivated state, it may be desirable to recover some activity by regenerating the catalyst. Two different regeneration

Table 1
Regeneration with air at 80 h compared to performance at 30 h.

Parameter	After 30 h	Before regeneration at 80 h	After regeneration at 80 h
H ₂	18.1%	14.3%	16.8%
CO	19.6%	18.2%	20.8%
CO ₂	4.0%	3.9%	2.9%
CH ₄	0.77%	0.76%	0.73%
Fuel conversion	73%	67%	74%

methods were attempted: (1) a high temperature regeneration following reactor shutdown after 80 h of operation and (2) a low temperature regeneration after 370 h of operation. The regeneration after 80 h was obtained by reintroducing air into the reactor immediately after shut down, before the catalyst cooled down (measured reactor temperatures were between 425 and 800 °C). During this procedure the steam flow rate was maintained at its original set point. When air was introduced, a temperature increase was measured which started in the center of the catalyst bed (which had been at 790 °C) and propagated downstream. A calculation of the residence time of steam in the reactor showed that any residual fuel left in the reactor would have been swept out of the reactor before the air was reintroduced – for a flow rate of 30 SLPM and a reactor volume of 30 cm³ the residence time was 60 ms whereas the time delay between fuel shutdown and air introduction was 10 s. The observed temperature wave is likely due to oxidation of carbon that had deposited on the catalyst surface. At this time, while no other product species (CO, H₂, CH₄) were measured in the reactor exhaust, CO₂ was detected and measured to be 3.8 times the measured value of CO₂ in the absence of reaction (when only air and steam are introduced into the reactor). This is aligned with carbon deposition behavior observed in literature. It has been reported that in ATR oxygen is depleted in the upstream region [29] and H₂O concentrations decrease in the axial direction [28]. Therefore, since coke is more likely to form at lower H₂O or O₂ concentrations [22], it is expected that carbon deposition would start in the middle of the reactor and continue downstream. After the reactor was re-started, JP8 conversion was higher than at the time of shutdown and H₂ and CO concentrations had increased, as shown in Table 1. The conversion measured after regeneration was the same as the conversion measured after 30 h of operation; however, the product distribution was different, indicating that while fuel conversion had been recovered, the catalyst was not in the same state it was in after 30 h of operation. This could indicate that different deactivation mechanisms are taking place which affect different reactions, and while the full activity (as of 30 h) has been recovered with respect to conversion, other reactions are still not occurring to the same extent. Since CO selectivity was higher after regeneration and the CO₂ concentration did not significantly increase, it is possible that irreversible deactivation has selectively poisoned sites for CO oxidation. Therefore, sites for steam reforming may have been recovered (hence higher H₂ and CO) but further oxidation of the CO to CO₂ did not take place.

Following 370 h of testing, regeneration was attempted by operating under fuel-lean conditions. The air flow rate was kept close to nominal conditions and flow rates of steam and fuel were adjusted in order to achieve reactor temperatures of ~700 °C. Regeneration is often done with pure air at temperatures of 600–700 °C since this is the temperature range where coke is oxidized [30]. This requires a large energy input for heating of the air, but allows for a large concentration gradient in order to remove poisons from the catalyst surface. Fuel-lean regeneration is advantageous because it does not require significant pre-heating of the mixture, since the oxidation of the fuel can provide the heat; however, there will be sulfur in the gas phase which decreases the driving force for desorption of sulfur (or sulfur compounds) from the catalyst surface if sulfur des-

Table 2

Regeneration under fuel-lean combustion conditions after 370 h of ATR with 125 ppm sulfur in fuel.

Parameter	After 370 h	1st regeneration (1.5 h)	2nd regeneration (1.5 h)
H ₂	12.2%	14.4%	15.0%
CO	18.8%	20.4%	20.5%
CO ₂	2.4%	2.7%	2.7%
CH ₄	0.85%	0.64%	0.68%
Fuel conversion	64%	72%	73%

orption takes place during regeneration. Additionally, in the case of ATR, a furnace is not usually present to heat the reactor since it is not needed during normal operation. Therefore, regenerating without a furnace provides a practical solution for high temperature regeneration in an ATR.

The reactor was operated under regeneration conditions for 1.5 h and then returned to nominal ATR conditions. Following steady state measurements of product concentrations, regeneration was again attempted (for 3 h), and then the system was returned to nominal ATR operation. Concentrations of product species and fuel conversion are shown in Table 2. After the first attempted regeneration for 1.5 h H₂ and CO concentrations increased by 2.3% and 1.6% from initial concentrations of 12.2% and 18.8%, respectively. The second attempted regeneration showed very slight (<1%) increases in H₂ and CO concentrations. Since fuel-lean operation for a longer period of time resulted in only a slight increase in activity, it is likely that this method will not achieve initial catalyst activity in a reasonable amount of time. While this extent of regeneration is not necessarily practical, it resulted in some change in the state of the catalyst, as evidenced by the increase in performance. It is interesting to note that the selectivity after this regeneration was not the same as the regeneration after 80 h. After 80 h, regeneration recovered equal amounts of CO and H₂, while the regeneration with fuel had a bigger impact on H₂ concentration than on CO concentration. This may indicate that different deactivation mechanisms are taking place where some are reversible and some are not. Therefore, the activity recovered from regeneration is a combination of the activity gained by the regeneration and the activity lost over the total time of operation via non-reversible deactivation. This presents a direction for future work in order to understand and isolate different deactivation mechanisms.

3.5. Comparison of 125 ppm sulfur and sulfur-free fuel

In order to elucidate the effects of sulfur on ATR reactions, we compare the results of the durability tests in the presence and absence of sulfur. Temperature profiles for ATR with sulfur-free and 125 ppm sulfur fuel are shown in Fig. 10. Fig. 10A shows data 3 h after catalyst light-off where temperature profiles match within 3%, throughout the reactor. Fig. 10B shows data after 80 h. While front end reactor temperatures match, the temperature profiles in the downstream part of the catalyst bed differ. The reactor exit temperature had risen from 644 °C to 733 °C when sulfur was present, and decreased from 634 °C to 601 °C in the absence of sulfur. It has been shown that oxygen gets fully converted in the front end of the catalyst bed, therefore oxidation reactions take place upstream while most water consuming reactions take place throughout the reactor (except for at the front end, where water may be produced by complete oxidation) [29]. If sulfur induced deactivation affects the activity of the reforming reactions, it is expected that the downstream reactor temperature would increase. Fig. 10 shows that after 80 h of operation the exit temperature was 130 °C higher with sulfur-containing fuel compared to sulfur free fuel. A calculation was done in order to predict the temperature decrease if deactiva-

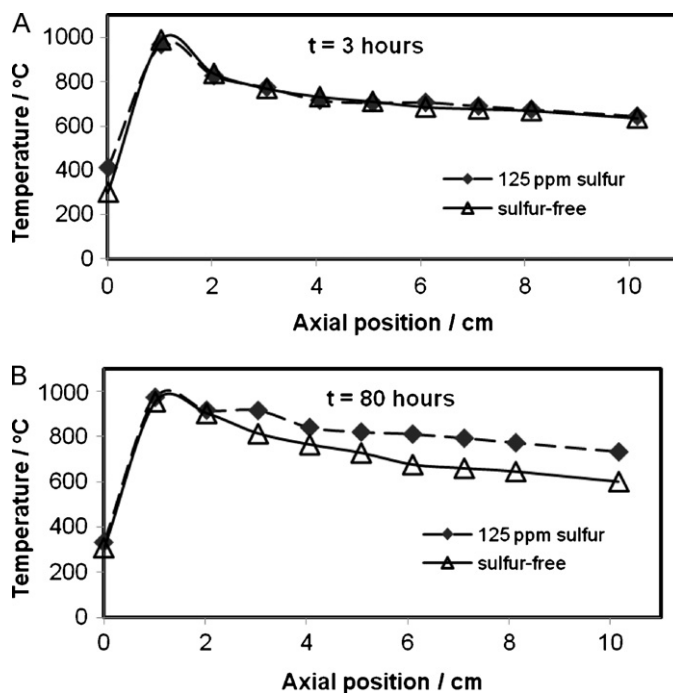


Fig. 10. Axial temperature profiles for fuel in the presence and absence of sulfur after (A) 3 h; (B) 80 h. At 80 h reactor exit temperature with sulfur is 130 °C higher than without sulfur, indicating that sites for endothermic reforming reactions have been poisoned.

tion selectively poisons the sites for steam reforming of the fuel. The calculation was done by modeling a reactor whose initial composition is equal to that of the sulfur free mix after 80 h and whose initial temperature is equal to the reactor exit temperature after 80 h (733 °C). It was then assumed that steam reforming of fuel took place and the extent of reaction was determined based on the difference in fuel conversion between the sulfur free fuel and the fuel with 125 ppm of sulfur at 80 h. An adiabatic temperature calculation was done based on a basic heat balance that equates heat released from reaction to the product of mass flow rate, heat capacity and temperature change. This calculation predicted a temperature change of 195 °C; in other words, if we apply the steam reforming reaction to the sulfur-containing mixture then the temperature would decrease by 195 °C in an adiabatic system. In the context of this ATR system, this indicates that if we start from the sulfur-free conditions and the steam reforming reaction is turned off (deactivation) such that all measured loss in fuel conversion is due to loss in steam reforming reaction (of the fuel) then one would expect the temperature to rise by 195 °C. The experiments showed a temperature difference of 130 °C between the sulfur-free fuel and the fuel containing sulfur. It has been suggested in literature that the fuel cracks and these cracked products undergo steam reforming reactions rather than the fuel directly reacting with steam. If we perform the same enthalpy calculation with a smaller hydrocarbon, for example n-heptane, the calculated temperature difference is 130 °C (the number of moles of hydrocarbon reactant was kept constant, so we now assume 1 mole of n-heptane per mole of JP8). Since temperature calculations for cracked products gives a closer temperature estimate, this may indicate that steam reforming does in fact occur with cracked hydrocarbons rather than with the fuel itself. In literature it has also been observed that steam reforming reactions are impacted most significantly by sulfur deactivation. Rabe et al. modeled catalytic reforming of gasoline and found that the presence of sulfur has a greater impact on steam reforming of higher hydrocarbons than on WGS or CH₄ reforming reactions [28]. Mayne et al. observed that the presence

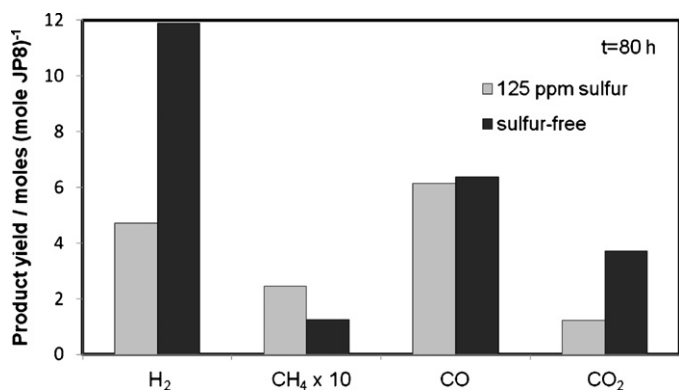


Fig. 11. Product yields after 80 h of ATR with sulfur-free fuel and 125 ppm of sulfur fuel.

of thiophene during ATR of isooctane had a greater impact on the steam reforming reactions than the partial oxidation reactions [31].

Product distributions can also provide information on the deactivation mechanisms taking place. The CH₄ concentration decreased over time with sulfur-free fuel, and increased when sulfur was present. This could be a result of a decrease in CH₄ reforming reactions. It has been shown that CH₄ is likely formed in the reactor via methanation reaction (Eq. (6)) and cracking reactions [26]; however, it may be consumed downstream by reforming reactions. Therefore, the sulfur deactivation may be affecting the downstream reforming reaction more than the upstream methanation/cracking reaction. A plot of product yields for both fuels at 80 h is shown in Fig. 11. CO yield is the same for the two fuels; H₂ yield for fuel with sulfur is 40% of the yield with sulfur-free fuel and CO₂ yield is 33% of the value obtained without sulfur. Since the fuel conversion is higher for sulfur-free fuel (93% compared to 67% with sulfur), it is surprising that both have the same CO yield. This could be explained in two ways; either both produce the same amount of CO and the deactivation only affects CO₂ producing reactions, or more CO may be formed without sulfur (resulting in higher conversion), which later gets converted downstream to CO₂, for example, via the water gas shift reaction. Since the mechanism for CO₂ formation often involves first the formation of CO and then conversion to CO₂, it is likely that sulfur selectively poisons catalyst sites for CO oxidation.

4. Conclusions

The data presented here shows that the catalyst used was not affected by cycling; the startup and shutdown procedure did not impact catalyst performance with respect to measured product concentrations (H₂, CO, CO₂, CH₄) or reactor temperatures. This indicates that thermal cycling and introduction of fuel at 300 °C does not affect catalyst performance. The catalyst demonstrated slight deactivation over 80 h of operation with sulfur-free fuel which is reflected by a 7% decrease in fuel conversion and 13% decrease in H₂ concentration. It is likely that the deactivation observed is due to a loss in WGS activity. While temperature throughout the reactor changes by over 300 °C, the front end reactor temperature is important in determining final product distribution, specifically for oxidized carbon species. ATR with fuel containing sulfur demonstrated higher CO selectivity and lower H₂ concentrations and conversion. Stable catalyst activity was achieved after 250 h of operation and maintained for over 100 h. Regeneration of the catalyst was demonstrated, but initial activity and selectivity were not achieved. Comparison of results with and without sul-

fur indicated that sulfur deactivation likely affects steam reforming reactions, which was reflected by an increase in reactor exit temperature with sulfur present which was not observed in the absence of sulfur. CH₄ concentrations increased with sulfur present and decreased in the absence of sulfur, indicating that it is likely that CH₄ reforming takes place in the reactor and is impacted by the presence of sulfur. Additionally, product yields showed that sulfur likely affects the carbon species selectivity by deactivating sites which contribute to the oxidation of CO.

Acknowledgements

The authors would like to thank ATK/GASL (Ronkonkoma, NY) for supporting this research and BASF Catalysis LLC (Iselin NJ) for providing the catalyst. The authors thank Florin Girlea (ATK) and Amy Knorpp for contributions to the experimental work presented here. We would like to thank Bob Farrauto (BASF) for insightful discussions throughout this project.

References

- [1] I. Aartun, B. Silberova, H. Venvik, P. Pfeifer, O. Gorke, K. Schubert, A. Holmen, *Catalysis Today* 105 (2005) 469–478.
- [2] S. Ahmed, M. Krumpelt, *International Journal of Hydrogen Energy* 26 (2001) 291–301.
- [3] B.D. Gould, X.Y. Chen, J.W. Schwank, *Journal of Catalysis* 250 (2007) 209–221.
- [4] L. Dorazio, M.J. Castaldi, *Catalysis Today* 136 (2008) 273–280.
- [5] F. Barrai, M.J. Castaldi, *Industrial & Engineering Chemistry Research* 49 (2010) 1577–1587.
- [6] O. Ilinich, W. Ruettinger, X.S. Liu, R. Farrauto, *Journal of Catalysis* 247 (2007) 112–118.
- [7] X.S. Liu, W. Ruettinger, X.M. Xu, R. Farrauto, *Applied Catalysis B: Environmental* 56 (2005) 69–75.
- [8] B.D. Gould, A.R. Tadd, J.W. Schwank, *Journal of Power Sources* 164 (2007) 344–350.
- [9] M. Ferrandon, J. Mawdsley, T. Krause, *Applied Catalysis A: General* 342 (2008) 69–77.
- [10] S. Gudlavalleti, T. Ros, D. Liefstink, *Applied Catalysis B: Environmental* 74 (2007) 251–260.
- [11] X.Y. Chen, B.D. Gould, J.W. Schwank, *Applied Catalysis A: General* 356 (2009) 137–147.
- [12] C.H. Bartholomew, *Applied Catalysis A: General* 212 (2001) 17–60.
- [13] P.K. Cheekatamarla, A.M. Lane, *Journal of Power Sources* 152 (2005) 256–263.
- [14] X. Karatzas, M. Nilsson, J. Dawody, B. Lindström, L.J. Pettersson, *Chemical Engineering Journal* 156 (2010) 366–379.
- [15] K.W. Smith, S.R. Proctor, A. Ozonoff, M.D. McClean, *Journal of Occupational and Environmental Hygiene* 7 (2010) 563–572.
- [16] United States Department of Defense: Turbine Fuel, Aviation, Kerosene Type, JP-8 (NATO F-34), NATO F-35, and JP-8+100 (NATO F-37). Ohio: USDoD, 2010. Available online.
- [17] D.J. Liu, T.D. Kaun, H.K. Liao, S. Ahmed, *International Journal of Hydrogen Energy* 29 (2004) 1035–1046.
- [18] R.K. Kaila, A.O.I. Krause, *International Journal of Hydrogen Energy* 31 (2006) 1934–1941.
- [19] B.J. Dreyer, I.C. Lee, J.J. Krummenacher, L.D. Schmidt, *Applied Catalysis A: General* 307 (2006) 184–194.
- [20] A. Qi, S. Wang, C. Ni, D. Wu, *International Journal of Hydrogen Energy* 32 (2007) 981–991.
- [21] I. Kang, J. Bae, G. Bae, *Journal of Power Sources* 163 (2006) 538–546.
- [22] M. Flytzani-Stephanopoulos, G.E. Voecks, *International Journal of Hydrogen Energy* 8 (1983) 539–548.
- [23] I.C. Lee, *Catalysis Today* 136 (2008) 258–265.
- [24] P.K. Cheekatamarla, A.M. Lane, *International Journal of Hydrogen Energy* 30 (2005) 1277–1285.
- [25] J. Pasel, J. Meißner, Z. Pors, R.C. Samsun, A. Tschauder, R. Peters, *International Journal of Hydrogen Energy* 32 (2007) 4847–4858.
- [26] A.D. Qi, S.D. Wang, G.Z. Fu, D.Y. Wu, *Applied Catalysis A: General* 293 (2005) 71–82.
- [27] S. Nair, B.J. Tatarchuk, *Fuel* 89 (2010) 3218–3225.
- [28] S. Rabe, F. Vogel, T.-B. Truong, T. Shimazu, T. Wakasugi, H. Aoki, H. Sobukawa, *International Journal of Hydrogen Energy* 34 (2009) 8023–8033.
- [29] Y.Y. Hu, D.J. Chmielewski, D. Papadakis, *Industrial & Engineering Chemistry Research* 47 (2008) 9437–9446.
- [30] A. Shamsi, J.R. Baltrus, J.J. Spivey, *Applied Catalysis A: General* 293 (2005) 145–152.
- [31] J.M. Mayne, A.R. Tadd, K.A. Dahlberg, J.W. Schwank, *Journal of Catalysis* 271 (2010) 140–152.